

Noble Gas Compounds and Chemistry

Theoretical Prediction on the New Types of Noble Gas Containing Anions OBONgO⁻ and OCNNgO⁻ (Ng = He, Ar, Kr and Xe)

Cheng-Cheng Tsai, Yu-Wei Lu and Wei-Ping Hu*

Department of Chemistry and Biochemistry, National Chung Cheng University, Chia-Yi 621, Taiwan

*Correspondence: chewph@ccu.edu.tw; Tel.: +886-5-272-0411 (ext. 66402)

Abstract: The fluorine-less noble-gas containing anions OBONgO⁻ and OCNNgO⁻ have been studied by correlated electronic structure calculation and density functional theory. The obtained energetics indicates that for Ng = Kr and Xe, these anions should be kinetically stable at low temperature. The molecular structures and electron density distribution suggests that these anions are stabilized by ion-induced dipole interactions with charges concentrated on the electronegative OBO and OCN groups. The current study shows that in addition to the fluoride ion, polyatomic groups with strong electronic affinities can also form stable noble-gas containing anions of the type X⁻...NgO.

Keywords: Noble Gas Anions; Noble Gas Chemistry; Electron Density; Stability of Noble-Gas Containing Molecules

1. Introduction

Noble gas (Ng) atoms contain completely filled valence shells and thus do not participate the normal chemical bonding that the other main group atoms do. Studies since 1960s, however, have shown that noble gases do form chemical compounds with very electronegative atoms and groups, such as in XePtF₆[1], XeF₂[2], XeF₄[3], XeO₄[4], etc. From 1980s, chemists have successfully made various noble gas hydrides HNgX in noble-gas matrixes at cryogenic condition[5-9], including the only known neutral argon-containing molecules HArF[6]. In recent years, new experimental techniques and computational studies have discovered and predicted many new types of noble-gas containing molecules, and the field of noble-gas chemistry has been flourishing[10-15].

Since the inertness of noble gases derives from the filled valence electrons, it is not surprising that varieties of noble-gas containing cations can be made, such as [UO₂(Ng)_n]⁺[16], HNgFNgH⁺[17], HNgCS⁺[18] and HNgCCO⁺[19], etc. On the other hand, the formation of noble-gas containing anions are expected to be more difficult since there are “too many” electrons in noble gases for chemical bonding already. However, several types of stable anions have been predicted such as FNgO⁻[20], FNgBN⁻[21], FNgCC⁻[22],

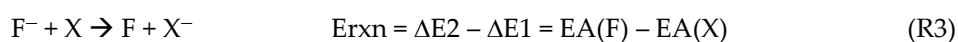
NNgO₃⁻[23], [NgBeB₁₁(CN)₁₁]²⁻[24], [B₁₂Ng₁₂F₁₂]²⁻[25], XAuNgX⁻ [26] and FNgS⁻[27].

Through some inductive effects, the binding of the excess electrons and the chemical bonding is surprisingly strong. It thus seems that there is rich anionic noble gas chemistry after all.

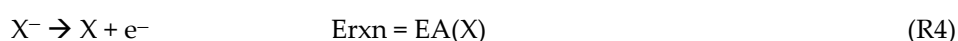
For the FNgX⁻ (X = O, BN, CC) anions, the stability comes from the ion induced dipole interaction. That is, the high charge density of the fluoride ion strengthens the NgX bonding with significant electron density transfer from the noble gas atom to the X group, while the fluorine atom remains its anionic character. The three-body dissociation of FNgX may proceed through two reactions:



and the difference in the energies of reaction (Er_{xn}) is just the difference of the electron affinity (EA) between F and X :



where EA(X) is defined by



From a previous computational study on FHeO⁻[20], $\Delta E_1 = 20.5$ kcal/mol, $\text{EA}(\text{F}) - \text{EA}(\text{O singlet}) = -4.7$ kcal/mol, and thus $\Delta E_2 = 15.9$ kcal/mol. It is interesting to know whether other atomic or polyatomic anions Y⁻ can replace the fluoride and also form stable anion YNgX⁻. From above, the Y⁻ must have strong polarizing effects with charge concentrated on a small atom (O, N) to give a relatively large ΔE_1 . In addition, Y must have an EA larger or comparable to that of X, otherwise the R2 could become a fast dissociation channel due to the low energy of reaction (ΔE_2). The OCN and OBO are isoelectronic groups with very high electron affinities. In the current study, we investigated whether these groups can form stable noble-gas containing anion (OBO⁻...NgO, OCN⁻...NgO, NCO⁻...NgO) and analyzed their molecular structures and chemical bonding.

2. Methods

Molecular geometry and harmonic vibrational frequencies were calculated using the MP2 theory[28] with the aug-cc-pVDZ and aug-cc-pVTZ basis sets[29-30]. They were also obtained using the B3LYP[31] and MPW1B95[32] hybrid density functional theory with aug-cc-pVTZ basis set. Single-point energy calculation was also performed using the CCSD(T) theory[33] with the aug-cc-pVTZ and aug-cc-pVQZ basis sets to acquire more accurate relative energies. For the Ar atom, the related basis sets aug-cc-pV(D+d)Z, aug-cc-pV(T+d)Z, and aug-cc-pV(Q+d)Z[34] were used ; and for the Xe atom, the basis sets aug-cc-pVDZ-pp,

aug-cc-pVTZ-pp, and aug-cc-pVQZ-pp[35] were used where the inner 28 electrons were replaced by a relativistic pseudopotential. In the rest of this article, the basis sets will be abbreviated as apn_z ($n = d, t, q$). The electron density distribution and ChelpG atomic charges[36] were obtained at the MP2/aug-cc-pVDZ level. All the electronic structure calculation was performed using Gaussian 09 program rev. D01[37].

3. Results and Discussion

3.1 Structures

Calculated structures of $OBONgO^-$ ($Ng = He, Ar, Kr, Xe$) at MP2/aptz level are shown in Figure 1. Structures obtained at other theoretical levels are included in the supplementary materials. Interestingly, for $Ng = He$ and Xe the predicted structures are bent, but for Ar and Kr the calculated structures are linear. This is due to the very small force constants along the $Ng-O-B$ angle where the $Ng-OBO$ bonding is mainly ionic. This will be discussed later in this article. Structures predicted by B3LYP and MPW1B95 density functional theory are all nonlinear. In all calculated bent conformation, the $Ng-O-B$ angles were predicted from 120 to 135 degrees. The terminal $Ng-O$ distances were predicted to be 1.064–1.899 Å, which are quite short and correlate well with the sizes of the noble gas atoms. They are similar to the $Ng-O$ distances in the $FNgO^-$ anions from a previous study[20]. The $Ng-OBO$ distance were predicted from 1.852 to 2.509 Å. It is noted that this distance increases only slightly (0.05 Å) from $OBOArO^-$ to $OBOXeO^-$, which is consistent that the bonding is ionic in nature. Thus the structures are better represented as $[OBO...Ng=O]^-$. In all cases, the $O-B$ distance on the noble gas side is slightly (0.01–0.02 Å) longer than the distance on the other side. Both distances are very close to the $O-B$ distance (1.275 Å) in OBO^- .

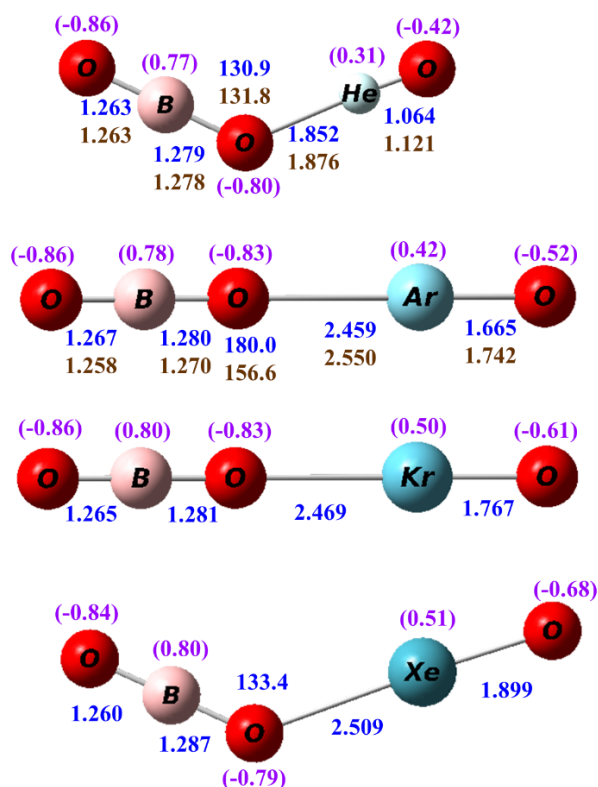


Figure 1. Calculated structures of OBONgO^- ($\text{Ng} = \text{He, Ar, Kr}$ and Xe). The bond distances are in angstroms and bond angles in degrees. The numbers in blue and brown are values calculated by MP2/aptz and CCSD(T)/aptz methods, respectively. The values in purple are CHelpG atomic charges.

Calculated structures of OCNNgO^- ($\text{Ng} = \text{He, Ar, Kr, Xe}$) at MP2/aptz level are shown in Figure 2. Structures obtained at other theoretical levels are also included in the supplementary materials. All predicted structures are planar and bent except for OCNHeO^- which is linear. Structures predicted by density functional theory are all nonlinear. The predicted terminal Ng-O distances are very similar to those in OBONgO^- . The N-Ng distances were predicted slightly longer (0.02–0.06 Å) than the corresponding O-Ng distances in OBONgO^- . This distance is also insensitive to the identity of the noble gas, and it increases only 0.02 Å from $\text{Ng} = \text{Ar}$ to $\text{Ng} = \text{Xe}$. The calculated C-N distances are slightly shorter (0.01–0.02 Å) than the O-C distances. Both distances are very similar to the corresponding bond distance ($\text{O-C} = 1.233$ Å, $\text{C-N} = 1.204$ Å) in OCN^- .

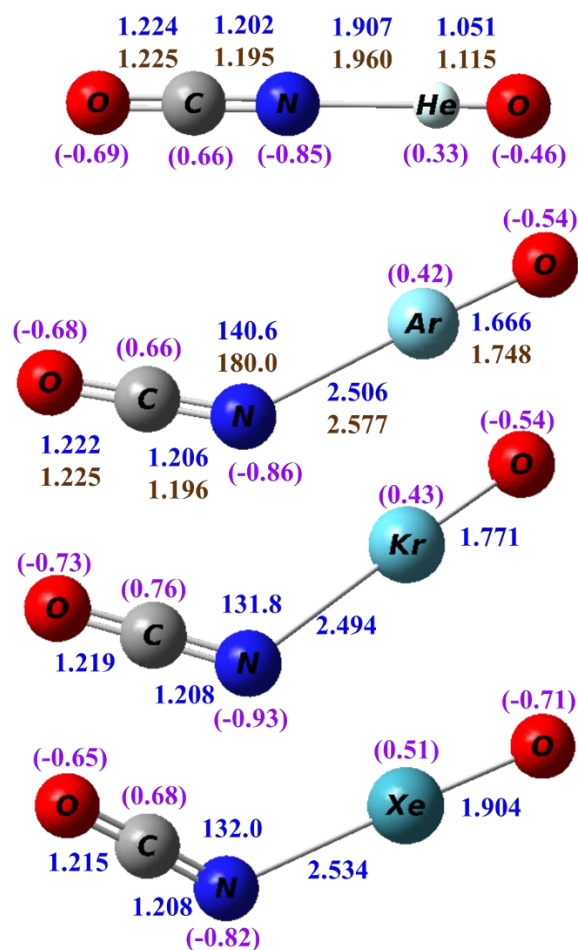


Figure 2. Calculated structures of OCNNGO^- ($\text{Ng} = \text{He, Ar, Kr}$ and Xe). The bond distances are in angstroms and bond angles in degrees. The numbers in blue and brown are values calculated by MP2/aptz and CCSD(T)/aptz methods, respectively. The values in purple are CHelpG atomic charges.

The structures of the isomeric NCONgO^- are shown in Figure 3. All predicted structures are planar and bent. In NCONgO^- the predicted differences in the C-N and C-O distances are more significant with the C-O distances 0.04–0.05 Å longer. As compare to OCNNGO^- , the O-C distances are 0.02–0.03 Å longer, the C-N distances ~0.01 Å shorter, and the terminal Ng-O distances are very similar.

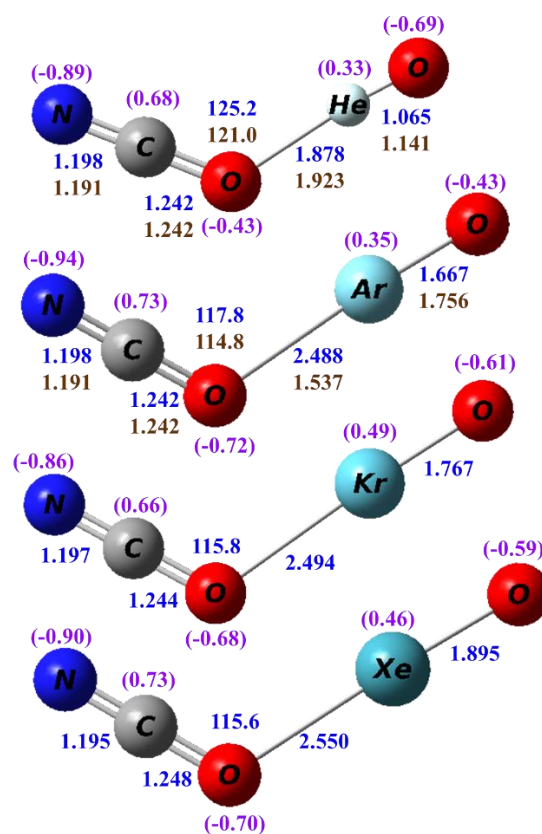


Figure 3. Calculated structures of NCONgO^- ($\text{Ng} = \text{He}, \text{Ar}, \text{Kr}$ and Xe). The bond distances are in angstroms and bond angles in degrees. The numbers in blue and brown are values calculated by MP2/aptz and CCSD(T)/aptz methods, respectively. The values in purple are CHelpG atomic charges.

The transition state (TS) structures for the two-body dissociation reactions $\text{OBONgO}^- \rightarrow \text{Ng} + \text{BO}_3^-$ are shown in Figure 4. Significant elongation of the $\text{OBO} \dots \text{Ng}$ distances relative to those in OBONgO^- are observed. For $\text{Ng} = \text{He}$ the NgO distance in TS also increases significantly. The Ng-O-B bond angles in the TS decrease to ~ 80 degrees except for $\text{Ng} = \text{He}$. Transition state structures for the two-body dissociation of OCNNgO^- are included in the supplementary materials.

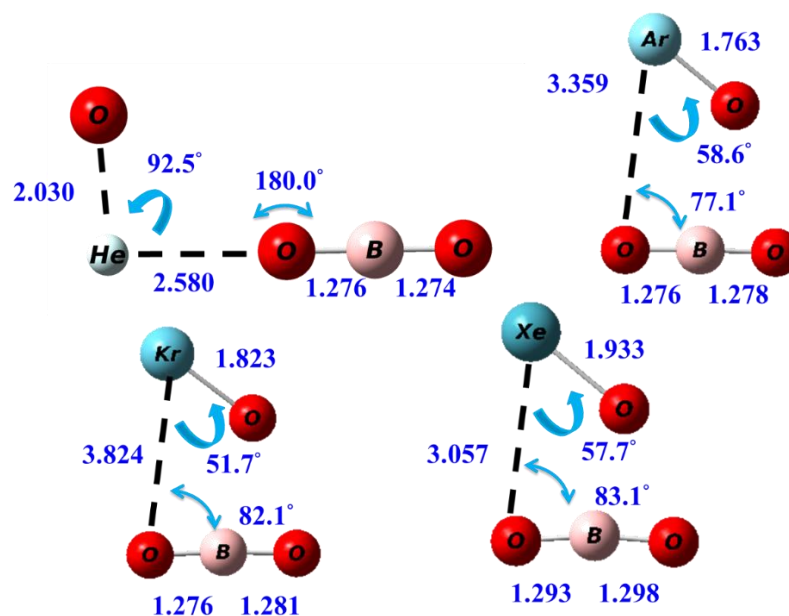


Figure 4. The calculated transition state structures of the two-body dissociation reactions of OBONgO⁻ at MP2/aptz level.

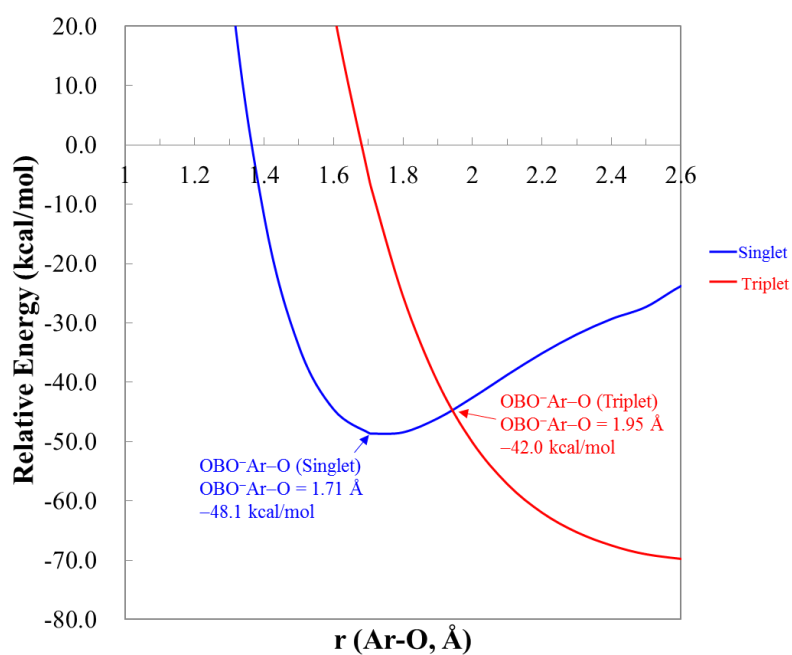


Figure 5. The singlet and triplet potential energy curves of OBOArO⁻ by extending the terminal Ar-O bond at CCSD(T)/aptz level. The zero of the energy is the total energy of a singlet oxygen atom, an OBO anion, and an argon atom.

3.2 Energetics

The predicted energies of reactions and dissociation barrier heights are listed in Table 1. The calculated electron affinities of O, OBO, and OCN at CCSD(T)/apqz level are 82.6, 105.8, and 83.8 kcal/mol, respectively. According to R1 to R4, the stability against the three-body dissociation of OBONgO⁻ and OCNNgO⁻ is determined by the reactions :



As shown in Table 1, the energy of reactions at CCSD(T)/apqz level for R5 are 7.4, 26.5, 43.6, and 67.4 kcal/mol for Ng = He, Ar, Kr, Xe, respectively. The values obtained at MP2/aptz level overestimate the stability by 13-21 kcal/mol, which is consistent with earlier studies[20, 22, 38-39]. The barrier heights of the two body dissociation at CCSD(T)/apqz level are 6-32 kcal/mol. The calculation thus indicates that for Ng = Ar, Kr, and Xe, the OBONgO⁻ are kinetically stable at low temperature, while for Ng = He, the anion is only marginally stable at the lowest temperature.

Table 1. The calculated three- and two-body dissociation energies, the two-body dissociation barriers, and the vertical singlet-triplet gaps of OBONgO⁻. All energies are Born–Oppenheimer energies in kcal/mol.

OBONgO ⁻	OBO ⁻ + Ng + O	Ng + BO ₃ ⁻	Barrier	S–T gap
Ng=He				
MP2/apdz	15.4	–96.7	13.6	82.5
MP2/aptz	19.8	–94.7	17.6	95.7
CCSD(T)/aptz ^a	6.1 [6.4]	–72.1 [–72.6]	5.2	91.7 [66.3]
CCSD(T)/apqz ^a	7.4	–70.3	6.4	80.2
Ng=Ar				
MP2/apdz	32.6	–79.5	21.2	39.4
MP2/aptz	41.3	–73.2	23.6	42.6
CCSD(T)/aptz ^a	25.5 [26.7]	–52.6 [–74.8]	18.1	41.1 [30.4]
CCSD(T)/apqz ^a	26.5	–51.2	18.5	41.3
Ng=Kr				
MP2/apdz	51.6	–60.4	28.0	50.5
MP2/aptz	60.7	–53.7	30.0	62.4
CCSD(T)/aptz ^a	42.5	–35.7	24.3	58.9
CCSD(T)/apqz ^a	43.6	–34.1	24.7	49.8

Ng=Xe				
MP2/apdz	76.2	-35.9	35.7	67.1
MP2/aptz	86.8	-27.6	37.6	69.2
CCSD(T)/aptz ^a	65.8	-12.3	31.9	55.5
CCSD(T)/apqz ^a	67.4	-10.3	32.4	55.4

^aSingle-point calculation using MP2/apdz structures. For Ng = He and Ar, energies in brackets are obtained using CCSD(T)/aptz structures.

The OCNNgO⁻ and NCONNgO⁻ are predicted to be very close in energies. All calculation predicts that OCNNgO⁻ are slightly lower in energies (data included in Supplementary Materials), and at CCSD(T)/apqz level the differences are only 2-4 kcal/mol. The interconversion reaction barriers from NCONNgO⁻ to OCNNgO⁻ were estimated to be only 1-4 kcal/mol. The interconversion TS structures and the reaction energetics are included in the supplementary materials. The predicted energies and barrier heights for the unimolecular dissociation reactions of OCNNgO⁻ are listed in Table 2. Predicted energetics for NCONNgO⁻ is included in supplementary materials. As shown in the Table, the energy of reactions at CCSD(T)/apqz level for R6 are 7.2, 26.5, 43.9, and 67.8 kcal/mol for Ng = He, Ar, Kr, and Xe, respectively. They are very similar to those for OBONNgO⁻. The barrier heights of the two body dissociation at CCSD(T)/aptz level are also very similar to those for OBONNgO⁻. Thus the OBONNgO⁻, OCNNgO⁻, and NCONNgO⁻ all have very similar kinetic stability. As compared to FNNgO⁻, these anions show higher stability against the three-body dissociation but slightly lower two-body dissociation barriers. As in the cases for FArO⁻, molecules with covalent ArO bonding are susceptible to intersystem crossing to the repulsive triplet state[20]. Figure 5 shows the calculated singlet and triplet potential energy curves along the terminal Ar-O bond of OBOArO⁻, and the crossing point is only approximately 6 kcal/mol above the singlet minimum, similar to that in FArO⁻. For Ng = Kr and Xe, the singlet-triplet energy gaps are predicted to be 15-23 kcal/mol, and they are less susceptible to the dissociation through intersystem crossing.

Table 2. The calculated three- and two-body dissociation energies, the two-body dissociation barriers, and the vertical singlet-triplet gaps of OCNNgO⁻. All energies are Born-Oppenheimer energies in kcal/mol.

OCNNgO ⁻	OCN ⁻ + Ng + O	Ng + NC(OO) ⁻	Barrier	S-T gap
Ng=He				
MP2/apdz	15.8	-55.7	14.0	85.9
MP2/aptz	17.4	-58.2	14.5	88.0
CCSD(T)/aptz ^a	6.6 [7.0]	-53.8 [-54.1]	5.6	115.6 [69.3]
CCSD(T)/apqz ^a	7.2	-53.1	11.4	89.4
Ng=Ar				
MP2/apdz	33.3	-38.3	22.1	41.1

MP2/aptz	42.3	-33.3	24.9	55.8
CCSD(T)/aptz ^a	26.2[27.3]	-34.2[-36.9]	19.1	42.6[34.4]
CCSD(T)/apqz ^a	26.5	-33.9	19.5	42.8
Ng=Kr				
MP2/apdz	53.1	-18.5	30.0	52.5
MP2/aptz	62.6	-13.3	32.1	64.5
CCSD(T)/aptz ^a	43.6	-16.8	26.3	51.3
CCSD(T)/apqz ^a	43.9	-16.4	26.6	51.4
Ng=Xe				
MP2/apdz	78.3	6.8	38.7	61.6
MP2/aptz	89.7	14.1	41.1	71.4
CCSD(T)/aptz ^a	67.0	6.4	34.1	56.8
CCSD(T)/apqz ^a	67.8	7.4	32.4	55.4

^aSingle-point calculation using MP2/apdz structures. For Ng = He and Ar, energies in brackets are obtained using CCSD(T)/aptz structures.

3.3 Electron Density

The ChelpG atomic charges for OBONgO⁻ are shown in Figure 1. The negative charge are clearly concentrated on the OBO groups. Plots of electron density distribution and Laplace concentration[40-42] are shown in Figures 6 and 7, respectively. The lack of electron density between the OBO and NgO groups suggests ionic interaction. The significant distortion in electron density along the bonding direction indicates that the Ng-O and O-B-O bonds are polar covalent[20-22,43-44]. The increasing polarity from He-O to Xe-O is also evident. Similar information is obtained from Figure 7 where electron concentration is seen between B-O (and, to a lesser extent, Ng-O), and electron depletion is observed between OBO and NgO. The depletion is less evident for the larger noble gases.

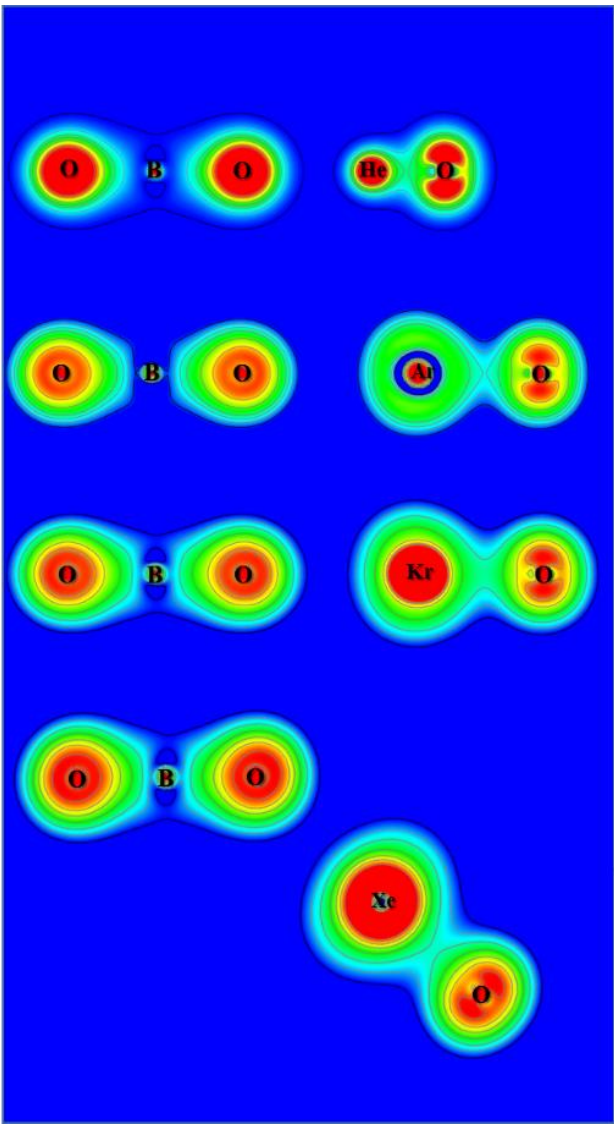


Figure 6. Contour plots of the calculated electron density of OBONgO[−].

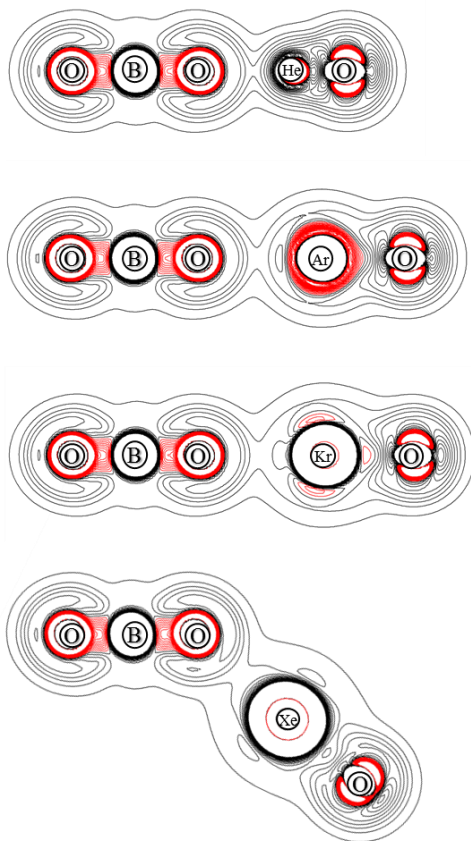


Figure 7. Contour plots of the calculated Laplace concentration of OBONgO^- . The red contour lines are in regions of charge concentration and the black contour lines are in regions of charge depletion.

From the calculated atomic charges for OCNNgO^- in Figure 2, the negative charges are also concentrated on the OCN groups. Plots of electron density distribution and Laplace concentration are shown in Figures 8 and 9, respectively. The lack of electron density between the OCN and NgO groups again suggests the interaction is ionic. Figure 8 shows that the polarity of $\text{O}-\text{C}$ is much stronger than $\text{C}-\text{N}$, as expected. Figure 9 shows significant charge concentration within the OCN groups, and the concentration region around $\text{C}-\text{N}$ is slightly larger than that around $\text{C}-\text{O}$. The atomic charges and electron density plots of NCONgO^- are included in the Supplementary Materials.

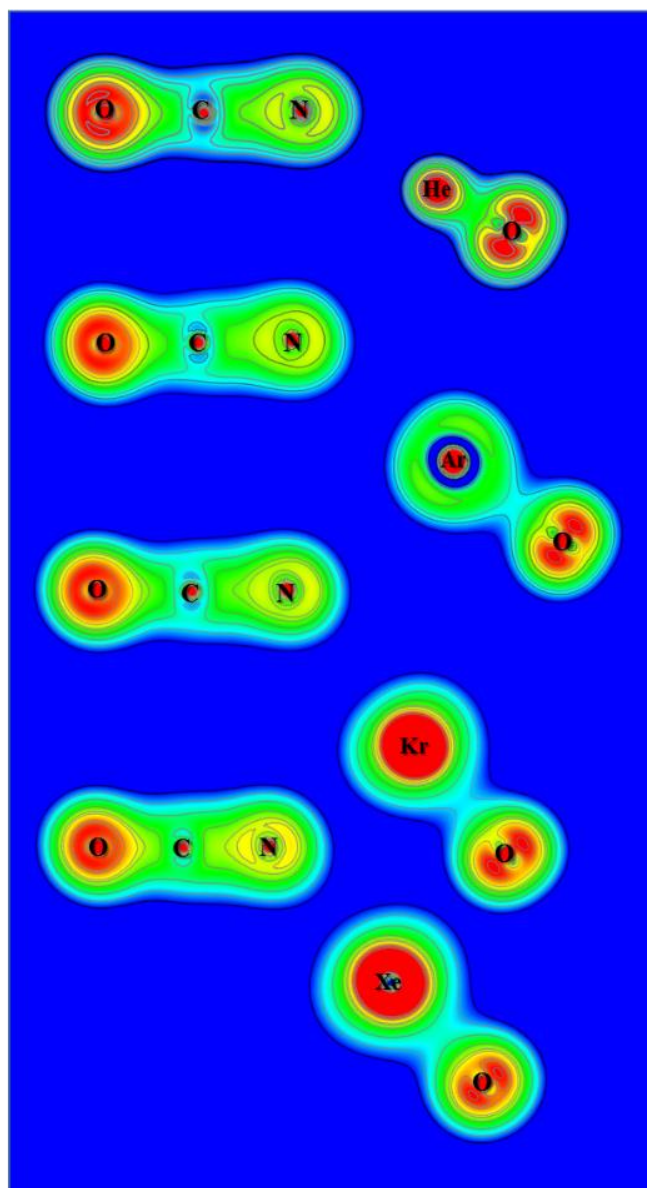


Figure 8. Contour plots of the calculated electron density of OCNNgO^- .

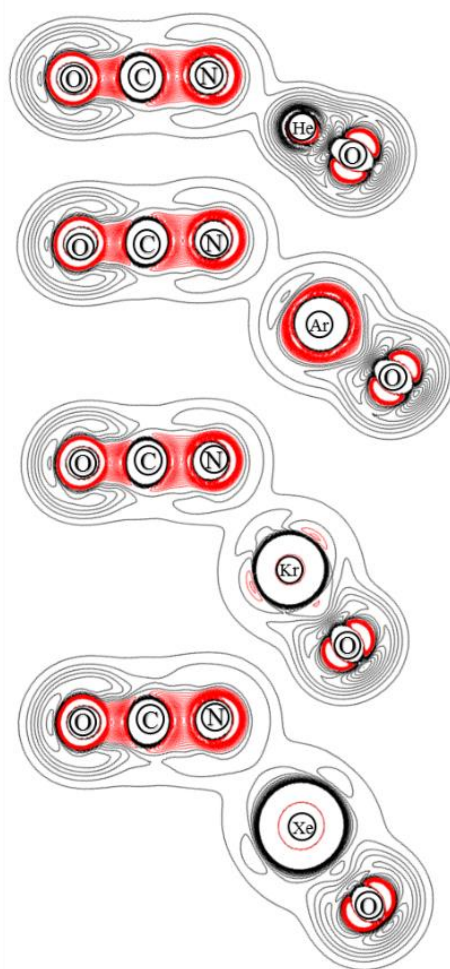


Figure 9. Contour plots of the calculated Laplace concentration of OCNNgO^- . The red contour lines are in regions of charge concentration and the black contour lines are in regions of charge depletion.

5. Conclusions

The anions OBONgO^- , OCNNgO^- , and NCONgO^- ($\text{Ng} = \text{He, Ar, Kr, Xe}$) have been studied by correlated electronic structure calculation. The results show that they are similar to FNgO^- with very short terminal NgO distances, and with the negative charge concentrated on the OBO (OCN , NCO) groups. The structures can conceptually be written as $\text{X}^- \dots \text{Ng}=\text{O}$ where the interaction between X and NgO is mostly ionic and the $\text{Ng}=\text{O}$ bonding is polar covalent. The anions are predicted to be kinetically stable for $\text{Ng} = \text{Ar, Kr, and Xe}$ on the singlet potential energy surface with the Ar -containing anions susceptible to intersystem crossing. The current study suggests that electronegative, fluorine-less chemical groups can form stable noble-gas containing anions through the ion-induced polarization, and these $\text{X}^- \dots \text{Ng}=\text{O}$ anions could be detectable in future experiments under cryogenic conditions.

Supplementary Materials

Supplementary materials, including tables of calculated relative energies, the two-body dissociation barriers, the vertical singlet-triplet gaps, two-body dissociation reactions transition state geometries by various theoretical methods can be accessed at:

Acknowledgments

This work is supported by the Ministry of Science and Technology (MOST) of Taiwan, R.O.C, Grant No. 109-2113-M-194-009. Part of computational resource is provided by National Center for High-performance Computing (NCHC).

References

- [1] Bartlett, N. Xenon hexafluoroplatinate (V) $\text{Xe}^+ [\text{PtF}_6]^-$ *Proc. Chem. Soc.* **1962**, 218.
- [2] Agron, P. A.; Begun, G. M.; Levy, H. A.; Mason, A. A.; Jones, C. G.; Smith, D. F. Xenon difluoride and the nature of the xenon-fluorine bond. *Science*. **1963**, 139, 842-844.
- [3] Claassen, H. H.; Selig, H.; Malm, J. G. Xenon tetrafluoride. *J. Am. Chem. Soc.* **1962**, 84, 3593-3593.
- [4] Selig, H.; Claassen, H. H.; Chernick, C. L.; Malm, J. G.; Huston, J. L. Xenon tetroxide: preparation and some properties. *Science*. **1964**, 143, 1322-1323.
- [5] Pettersson, M.; Lundell, J.; Khriachtchev, L.; Räsänen, M. J. Neutral rare-gas containing charge-transfer molecules in solid matrices. III. HXeCN , HXeNC , and HKrCN in Kr and Xe. *Chem. Phys.* **1998**, 109, 618-625.
- [6] Khriachtchev, L.; Pettersson, M.; Runeberg, N.; Lundell, J.; Rasanen, M. A stable argon compound. *Nature*. **2000**, 406, 874-876.
- [7] Pettersson, M.; Khriachtchev, L.; Lignell, A.; Räsänen, M.; Bihary, Z.; Gerber, R. J. HKrF in solid krypton. *J. Chem. Phys.* **2002**, 116, 2508-2515.
- [8] Khriachtchev, L.; Räsänen, M.; Gerber, R. B. Noble-gas hydrides: New chemistry at low temperatures. *Acc. Chem. Res.* **2009**, 42, 183-191.
- [9] Arppe, T.; Khriachtchev, L.; Lignell, A.; Domanskaya, A. V.; Räsänen, M. Halogenated Xenon Cyanides ClXeCN , ClXeNC , and BrXeCN . *Inorg. Chem.* **2012**, 51, 4398-4402.
- [10] Fernández, I.; Frenking, G. Neutral noble gas compounds exhibiting a Xe–Xe bond: structure, stability and bonding situation. *Phys. Chem. Chem. Phys.* **2012**, 14, 14869-14877.
- [11] Wang, Q.; Wang, X. Infrared Spectra of NgBeS ($\text{Ng} = \text{Ne}, \text{Ar}, \text{Kr}, \text{Xe}$) and BeS_2 in Noble-Gas Matrices. *J. Phys Chem. A*. **2013**, 117, 1508-1513.
- [12] Samanta, D. Prediction of superhalogen-stabilized noble gas compounds. *J. Phys. Chem. Lett.* **2014**, 5, 3151-3156.
- [13] Pan, S.; Jana, G.; Ravell, E.; Zarate, X.; Osorio, E.; Merino, G.; Chattaraj, P. K. Stable NCNgNSi ($\text{Ng} = \text{Kr}, \text{Xe}, \text{Rn}$) Compounds with Covalently Bound C–Ng–N Unit: Possible Isomerization of NCNSi through the Release of the Noble Gas Atom. *Chem. Eur. J.* **2018**, 24, 2879-2887.
- [14] Wu, L. Y.; Li, J. F.; Zhao, R. F.; Luo, L.; Wang, Y. C.; Yin, B. Exploring the structure, bonding and stability of noble gas compounds promoted by superhalogens. A case study on HNgMX_3 ($\text{Ng} = \text{Ar–Rn}$, $\text{M} = \text{Be–Ca}$, $\text{X} = \text{F–Br}$) via combined high-level ab initio and DFT calculations. *Phys. Chem. Chem. Phys.* **2019**, 21, 19104-19114.

- [15] Abdeveiszadeh, Z.; Noorizadeh, S. Theoretical investigation on the structure and stability of some neutral noble gas compounds containing Xe-Xe bond. *Int. J. Quantum Chem.* **2020**, *120*, e26185.
- [16] Wang, X.; Andrews, L.; Li, J.; Bursten, B. E. Significant Interactions between Uranium and Noble-Gas Atoms: Coordination of the UO_2^+ Cation by Ne, Ar, Kr, and Xe Atoms. *Angew. Chem. Int. Ed.* **2004**, *43*, 2554-2557.
- [17] Borocci, S.; Bronzolino, N.; Giordani, M.; Grandinetti, F. Cationic noble gas hydrides: a theoretical investigation of dinuclear HNgFNgH^+ ($\text{Ng} = \text{He}-\text{Xe}$). *J. Phys. Chem. A* **2010**, *114*, 7382-7390.
- [18] Ghosh, A.; Manna, D.; & Ghanty, T. K. Theoretical prediction of noble gas inserted thioformyl cations: HNgCS^+ ($\text{Ng} = \text{He, Ne, Ar, Kr, and Xe}$). *J. Phys. Chem. A* **2015**, *119*, 2233-2243.
- [19] Ghosh, A.; Gupta, A.; Gupta, R.; Ghanty, T. K. Noble gas hydrides in the triplet state: HNgCCO^+ ($\text{Ng} = \text{He, Ne, Ar, Kr, and Xe}$). *Phys. Chem. Chem. Phys.* **2018**, *20*, 20270-20279.
- [20] Li, T. H.; Mou, C. H.; Chen, H. R.; Hu, W. P. J. Theoretical prediction of noble gas containing anions FNgO^- ($\text{Ng} = \text{He, Ar, and Kr}$). *Am. Chem. Soc.* **2005**, *127*, 9241-9245.
- [21] Antoniotti, P.; Borocci, S.; Bronzolino, N.; Cecchi, P.; Grandinetti, F. Noble gas anions: a theoretical investigation of FNgBN^- ($\text{Ng} = \text{He}-\text{Xe}$). *J. Phys. Chem. A* **2007**, *111*, 10144-10151.
- [22] Peng, C. Y.; Yang, C. Y.; Sun, Y. L.; Hu, W. P. Theoretical prediction on the structures and stability of the noble-gas containing anions FNgCC^- ($\text{Ng} = \text{He, Ar, Kr, and Xe}$). *J. Chem. Phys.* **2012**, *137*, 194303.
- [23] Sun, Y. L.; Hong, J. T.; Hu, W. P. Theoretical Prediction of Stable Noble-Gas Anions XeNO_2^- and XeNO_3^- with very Short Xenon– Nitrogen Bond Lengths. *J. Phys. Chem. A* **2010**, *114*, 9359-9367.
- [24] Joshi, M.; Ghanty, T. K. Quantum chemical prediction of a superelectrophilic dianion and its binding with noble gas atoms. *ChemComm.* **2019**, *55*, 14379-14382.
- [25] Joshi, M.; Ghanty, T. K. Unprecedented stability enhancement of multiple charged anion through decoration with negative electron affinity noble gases. *Phys. Chem. Chem. Phys.* **2020**.
- [26] Guoqun, L.; Yanli, Z.; Xue, B.; Fang, H.; Xianxi, Z.; Zhixin, W.; Wangxi, Z. Theoretical investigation of the noble gas molecular anions XAuNgX^- and HAuNgX^- ($\text{X} = \text{F, Cl, Br}$; $\text{Ng} = \text{Xe, Kr, Ar}$). *Struct Chem.* **2012**, *23*, 1693-1710.
- [27] Borocci, S.; Bronzolino, N.; Grandinetti, F. Noble gas–sulfur anions: a theoretical investigation of FNgS^- ($\text{Ng} = \text{He, Ar, Kr, Xe}$). *Chem. Phys. Lett.* **2008**, *458*, 48-53.

- [28] Frisch, M. J.; Head-Gordon, M.; Pople, J. A. A direct MP2 gradient method. *Chem. Phys. Lett.* **1990**, *166*, 275-280.
- [29] Dunning Jr, T. H. Gaussian basis sets for use in correlated molecular calculations. I. The atoms boron through neon and hydrogen. *J. Chem. Phys.* **1989**, *90*, 1007-1023.
- [30] Dunning Jr, T. H.; Peterson, K. A.; Wilson, A. K. Gaussian basis sets for use in correlated molecular calculations. X. The atoms aluminum through argon revisited. *J. Chem. Phys.* **2001**, *114*, 9244-9253.
- [31] Stephens, P. J.; Devlin, F. J.; Chabalowski, C. F.; Frisch, M. J. Ab initio calculation of vibrational absorption and circular dichroism spectra using density functional force fields. *J. Phys. Chem.* **1994**, *89*, 11623-11627.
- [32] Zhao, Y.; Truhlar, D. G. Hybrid meta density functional theory methods for thermochemistry, thermochemical kinetics, and noncovalent interactions: the MPW1B95 and MPWB1K models and comparative assessments for hydrogen bonding and van der Waals interactions. *J. Phys. Chem. A.* **2004**, *108*, 6908-6918.
- [33] Purvis III, G. D.; Bartlett, R. J. A full coupled-cluster singles and doubles model: The inclusion of disconnected triples. *J. Chem. Phys.* **1982**, *76*, 1910-1918.
- [34] Dunning, T. H.; Peterson, K. A.; Wilson, A. K. J. Chem. Phys. Gaussian basis sets for use in correlated molecular calculations. X. The atoms aluminum through argon revisited. 2001, 114, 9244-9253.
- [35] Peterson, K. A.; Figgen, D.; Goll, E.; Stoll, H.; Dolg, M. Systematically convergent basis sets with relativistic pseudopotentials. II. Small-core pseudopotentials and correlation consistent basis sets for the post-d group 16-18 elements. *J. Chem. Phys.* **2003**, *119*, 11113-11123.
- [36] Breneman, C. M.; Wiberg, K. B. Determining atom-centered monopoles from molecular electrostatic potentials. The need for high sampling density in formamide conformational analysis. *J. Comput. Chem.* **1990**, *11*, 361-373.
- [37] Frisch, M. J.; Trucks, G. W.; Schlegel, H. B.; Scuseria, G. E.; Robb, M. A.; Cheeseman, J. R.; Scalmani, G.; Barone, V.; Mennucci, B.; Petersson, G. A.; Nakatsuji, H.; Caricato, M.; Li, X.; Hratchian, H. P.; Izmaylov, A. F.; Bloino, J.; Zheng, G.; Sonnenberg, J. L.; Hada, M.; Ehara, M.; Toyota, K.; Fukuda, R.; Hasegawa, J.; Ishida, M.; Nakajima, T.; Honda, Y.; Kitao, O.; Nakai, H.; Vreven, T.; Montgomery, Jr. J. A.; Peralta, J. E.; Ogliaro, F.; Bearpark, M.; Heyd, J. J.; Brothers, E.; Kudin, K. N.; Staroverov, V. N.; Kobayashi, R.; Normand, J.; Raghavachari, K.; Rendell, A.; Burant, J. C.; Iyengar, S. S.; Tomasi, J.; Cossi, M.; Rega, N.; Millam, J. M.; Klene, M.; Knox, J. E.; Cross, J. B.; Bakken, V.; Adamo, C.; Jaramillo, J.; Gomperts, R.; Stratmann, R. E.; Yazyev, O.;

- Austin, A. J.; Cammi, R.; Pomelli, C.; Ochterski, J. W.; Martin, R. L.; Morokuma, K.; Zakrzewski, V. G.; Voth, G. A.; Salvador, P.; Dannenberg, J. J.; Dapprich, S.; Daniels, A. D.; Farkas, Ö.; Foresman, J. B.; Ortiz, J. V.; Cioslowski, J.; Fox, D. J. gaussian 09, Revision d. 01, Gaussian. Inc., Wallingford CT, **2013**.
- [38] Chen, J. L.; Yang, C. Y.; Lin, H. J.; Hu, W. P. Theoretical prediction of new noble-gas molecules FN_gBNR (N_g = Ar, Kr, and Xe; R = H, CH₃, CCH, CHCH₂, F, and OH). *Phys. Chem. Chem. Phys.* **2013**, 15, 9701-9709.
- [39] Tsai, C. C.; Tsai, Z. Y.; Tseng, M. Y.; Hu, W. P. A new database and benchmark of the bond energies of noble-gas-containing molecules. *Int. J. Quantum Chem.* **2020**, e26238.
- [40] Hyndman, R. J. Computing and graphing highest density regions. *Am. Stat.* **1996**, 50, 120-126.
- [41] Matta, C. F.; Gillespie, R. J. Understanding and interpreting molecular electron density distributions. *J. Chem. Educ.* **2002**, 79, 1141.
- [42] Fux, S.; Kiewisch, K.; Jacob, C. R.; Neugebauer, J.; Reiher, M. Analysis of electron density distributions from subsystem density functional theory applied to coordination bonds. *Chem. Phys. Lett.* **2008**, 461, 353-359.
- [43] Thomas, J. M.; Walker, N. R.; Cooke, S. A.; Gerry, M. C. Microwave spectra and structures of KrAuF, KrAgF, and KrAgBr; ⁸³Kr nuclear quadrupole coupling and the nature of noble gas– noble metal halide bonding. *J. Am. Chem. Soc.* **2004**, 126, 1235-1246.
- [44] Lin, T. Y.; Hsu, J. B.; & Hu, W. P. Theoretical prediction of new noble-gas molecules OB_NgF (N_g = Ar, Kr, and Xe). *Chem. Phys. Lett.* **2005**, 402, 514-518.